

Thermal analysis of hexadecyltrimethylammonium-montmorillonites

Part 1. Thermogravimetry, carbon and hydrogen analysis and thermo-IR spectroscopy analysis

Isaak Lapides · Mikhail Borisover ·
Shmuel Yariv

ESTAC2010 Conference Special Issue
© Akadémiai Kiadó, Budapest, Hungary 2011

Abstract Na-montmorillonite (Na-MONT) was loaded with hexadecyltrimethylammonium cations (HDTMA) by replacing 41 and 90% of the exchangeable Na with HDTMA, labeled OC-41 and OC-90, respectively. Na-MONT, OC-41, and OC-90 were heated in air up to 900 °C. Unheated and thermally treated organoclays heated at 150, 250, 360, and 420 °C are used in our laboratory as sorbents of different hazardous organic compounds from waste water. In order to get a better knowledge about the composition and nature of the thermally treated organoclays Na-MONT and the two organoclays were studied by thermogravimetry (TG) in air and under nitrogen. Carbon and hydrogen contents in each of the thermal treated sample were determined and their infrared spectra were recorded. The present results showed that at 150 °C both organoclays lost water but not intercalated HDTMA cations. At 250 °C, many HDTMA cations persisted in OC-41, but in OC-90 significant part of the cations were air-oxidized into H₂O and CO₂ and the residual carbon formed charcoal. After heating both samples at 360 °C charcoal was present in both organo clays. This charcoal persisted at 420 °C but was gradually oxidized by air with further rise in temperature. TG runs under nitrogen showed stepwise degradation corresponding to interlayer water desorption followed by decomposition of the organic compound, volatilization of small fragments

and condensation of non-volatile fragments into quasi-charcoal. After dehydroxylation of the clay the last stages of organic matter pyrolysis and volatilization occurred.

Keywords Carbon content curves · Charcoal · Hydrogen content curves · Organo-montmorillonite · Thermo-infrared spectroscopy · Thermogravimetry

Introduction

Organoclay-based nanocomposites obtained by modifying Na-smectites with long chain surfactants are potential candidates for serving as sorbents of different organic molecules, as thickeners in paints, greases, oil-base drilling mud, for the purpose of gelling various organic liquids and as homogenizing fillers in the plastic industry [1–5]. They are also used in cleaning operations of drainage wastewater, oil-spill, etc. [6]. Some investigators claim that granular organoclays are more effective than activated carbon for removal of hazardous compounds from aqueous systems [7–9]. In recent years, our research has been focused on the effect of thermally treating the organoclay on its ability to adsorb toxic organic molecules found in drainage wastewater. In our research the clay mineral used hitherto for this purpose has been the swelling smectite clay mineral montmorillonite (MONT) and the surfactant has been the bromide salt of hexadecyltrimethylammonium (HDTMA, Scheme 1) [10]. The organoclay is prepared in aqueous systems by replacing the exchangeable Na⁺ with the organic cationic detergent HDTMA. In its natural state MONT is hydrophilic due to the presence of metallic cations in the interlayers. Loading MONT with a cationic surfactant converts the hydrophilic gallery surface into an organophilic surface [11].

I. Lapides · S. Yariv (✉)
Institute of Chemistry, The Hebrew University of Jerusalem,
Campus Edmund Y. Safra, 91904 Jerusalem, Israel
e-mail: yarivs@vms.huji.ac.il

M. Borisover
Institute of Soil, Water and Environmental Sciences, The Volcani Center, Agricultural Research Organization, POB 6, 50250 Bet Dagan, Israel



Scheme 1 Hexadecyltrimethyl ammonium cation (HDTMA), C₁₉H₄₂N

Two types of the organo-MONT used in our previous study were prepared by loading the clay with 41 and 90% of its cation exchange capacity (CEC) with HDTMA and were labeled OC-41 and OC-90, respectively [12, 13]. The unloaded Na-MONT and each organoclays sample were heated 2 h in ambient atmosphere at 150, 250, 360, and 420 °C and were used as sorbents [10]. In this study, in order to get a better knowledge about the composition and behavior of the thermally treated organoclays, samples were also heated at 550, 700, and 900 °C. Carbon and hydrogen contents in each of the thermal-treated sample were determined and their infrared spectra were recorded. As well, Na-MONT and the two organo-clays were studied by thermogravimetry (TG).

DTA and TG curves of Na-MONT (e.g. Wyoming bentonite) comprise two thermal stages: (1) evolution of intercalated and surface water, below ≈ 400 °C and (2) dehydroxylation of framework hydroxyls, above ≈ 400 °C [14, 15].

Previous simultaneous DTA-EGA (using mass spectrometry) showed that during the thermal analysis of organic-ammonium-MONT in air the adsorbed organic cation is oxidized in three steps. In the first step at about 250–350 °C most organic hydrogen is oxidized to water, but only some of the carbon and nitrogen are oxidized to CO₂ and NO₂, respectively. The remaining carbon and nitrogen with some hydrogen form charcoal sandwiched between the clay layers [16–18]. From DTA, EGA, and TG curves it was concluded that there exist two varieties of charcoal, one is oxidized at about 300–500 °C and the second at about 450–800 °C (second and third steps of oxidation) labeled low- and high-temperature stable charcoal, respectively [15, 19, 20].

The dehydroxylation of the clay is endothermic whereas the oxidation steps of the adsorbed organic are exothermic. In the presence of small amounts of organic matter, the third exothermic peak is sometimes overlapped by the dehydroxylation endothermic peak and is not detected in the DTA curve. On the contrary, in the presence of high amounts of organic matter the exothermic peak overlaps the dehydroxylation endothermic peak and the latter is not detected. In this case, the dehydroxylation temperature can be determined by EGA, using mass or infrared spectrometry.

From basal spacings of thermal-treated organoclays, it was deduced that the charcoal–MONT complexes contained mono- or bilayer carbon. In some cases the basal spacing was too small to account for an intercalated carbon monolayer and it was concluded that carbon atoms were

keying into the trigonal holes of the tetrahedral sheets [19]. Carbonization of organic matter in the interlayers of MONT was investigated by graphitizing polymers [21–24]. The black residue obtained at 700 °C was made from highly stacked films with small interplanar spacing of 0.337 nm. The formation of such a unique coke was attributed to the peculiar method where the two-dimensional space between the clay lamellae served as a unique field for carbonization.

He et al. [25] described the thermal analysis of HDTMA–MONT loaded with different amounts of the cation. Their DTA curves showed three exothermic peaks proving our previous suggestion of the existence of three oxidation steps [15, 17, 18].

Experimental

Materials

Bromide salt of HDTMA (99%) was purchased from Sigma-Aldrich. It was used without further purification. Wyoming bentonite (Na-MONT) with CEC of 90 meq/100 g was purchased from Fisher Scientific Company.

Methods

Preparation of the HDTMA-exchanged sorbents was previously described [12, 13]. In short, it involved (1) slow adding of the HDTMA bromide solution (0.03 M; 1.0–1.5 mL min⁻¹) to homogenized aqueous suspension of Wyoming bentonite (1.5%) during 5–6 h; (2) 15 h stirring; (3) centrifugation and determination of dissolved C in the supernatant; (4) sodium bromide was removed from the organo-clay complex by multiple washing with distilled water, until negative reaction with AgNO₃; (5) the thoroughly washed clay was freeze dried. Two different organoclays were synthesized with different loadings. They were labeled OC-41 and OC-90 whereas the number in the label indicates the extent of replacement of the exchangeable cation.

Thermogravimetric analyses

TG and DTG curves of 8–15 mg of Na-MONT, OC-41, and OC-90 were recorded from room temperature to 900 °C on a thermobalance Mettler Toledo TG50 analyzer. Measurements were performed at a heating rate of 10 °C/min. Parallel runs were carried out in air and in nitrogen atmosphere. The DTG curves of the organoclays measured in air were fitted in the temperature range 200–450 °C by using “Origin 7.0” program.

Carbon and hydrogen analyses

C and H contents of Na-MONT, OC-41, and OC-90 unheated and air-heated for 2 h at 150, 250, 360, 420, 550, 700, and 900 °C were determined at the Laboratory for Micro-Analysis of the Institute of Chemistry at the Hebrew University of Jerusalem by using a Perkin-Elmer-2400 C/H analyzer. 2–3 mg clay was used for each run. The results in mass percent were calculated on the basis of air-dried clay.

Thermo-FTIR spectroscopy

FTIR spectra of KBr disks (1.0 mg sample in 100.0 mg KBr) of the bromide salt of HDTMA and of OC-41 and OC-90 unheated and after heating them in air for 2 h at 150, 250, 360, and 420 °C were recorded on a Tensor-27 Bruker spectrometer.

Results and Discussion

He et al. [25] showed from DTA and TG runs in air (heated at 20 °C/min) that the oxidation of neat HDTMABr salt begins at ≈210 °C, and is accompanied by two exothermic peaks at 212 and 325 °C. From TG curve, the mass loss

corresponding to the two exothermic peaks accounts for 94%, indicating the formation of small amount of charcoal which is oxidized by air at ≈420–570 °C with an exothermic DTA peak at 473 °C. They also studied DTA and TG of HDTMA-modified MONT with different loadings of the organic cation between 0.2 and 5.0 times of the CEC. In agreement with our previous DTA-EGA study of organic ammonium MONTs the DTA curves of the modified MONTs showed three exothermic peaks above 200 °C attributed to three oxidation steps of the intercalated HDTMA cation [15–20].

From mass loss studied by He et al. (Table 1 in [25]), it appears that among the many HDTMA-MONTs which they synthesized, the samples prepared with initial surfactant concentrations of 0.5 and 1.5 times of the CEC of Na-MONT (with loadings of 46 and 93% of the CEC) were very similar to our OC-41 and OC-90, respectively, and consequently their DTA data (Fig. 2 in [25]) is reliable for the interpretation of our thermal analysis results.

Based on our previous DTA studies of organic-ammonium clays [15–20], it seems that the first exothermic peak in the DTA of HDTMA-MONT represents the first step of the thermal oxidation of the organic cation. At this step most of the organic hydrogen is oxidized into water, but only part of the carbon and nitrogen are oxidized into CO₂

Table 1 Data on CH₂, CH₃, and CC groups in infrared spectra of the neat surfactant [HDTMA]Br and of HDTMA-modified montmorillonites (OC-41 and OC-90) before thermal treatments and after heating the samples at 150, 250, 350, and 420 °C

Assignment	[HDTMA]Br	OC-41					OC-90				
		25 (°C)	150 (°C)	250 (°C)	360 (°C)	420 (°C)	25 (°C)	150 (°C)	250 (°C)	360 (°C)	420 (°C)
CH ₃ as	2960vw	2955sh	2955sh	2955sh	2960w	2965vw	2962t	2962t	2954sh	2963w	2969vw
CH ₃ as	2945w										
CH ₂ as	2918vi	2929vi	2929vi	2929i	2929w	2929w	2928i	2928vi	2931vi	2928vi	2923i
CH ₃ sym	2893t										
CH ₃ sym	2871vw						2873t	2871t	2871t	2875m	2872m
CH ₂ sym	2849i	2856i	2855i	2855m	2855w	2855w	2852vi	2851i	2859m	2854vi	2852vi
C–H def.	1487vi	1489i	1489i	1489i	1489vw	1489vw	1490i	1488i	1489vi	1489vw	1489vw
C–H def.	1474i	1475vi	1475vi	1475vi	1473w	1473 m	1474vi	1475vi	1475i	1474m	1474m
C–H def.	1462i	1459w	1459sh	1460sh							
CC str.					1457m	1456i			1458m	1457i	1457i
CC str.					1447m	1447vi			1447vw	1447i	1447i
CC str.					1437m	1436vi			1437w	1437vi	1437vi
C–H def.	1431m	1436vw	1436t	1436t							
CC str.					1420m	1420vi			1420w	1421i	1422i
C–H def.	1408m	1419m	1419w	1419w			1418w	1417w			
CC str.					1404sh	1404w				1404sh	
CC str.					1399sh	1399w			1397w	1399sh	1398w
C–H def.	1396m	1396vw									
CH ₂ def.	1383w										
CH ₂ def.	1361vw										

i intense, m medium, w weak, sh shoulder, t tail, v very, as asymmetric, sym symmetric, str. stretching, def. deformation

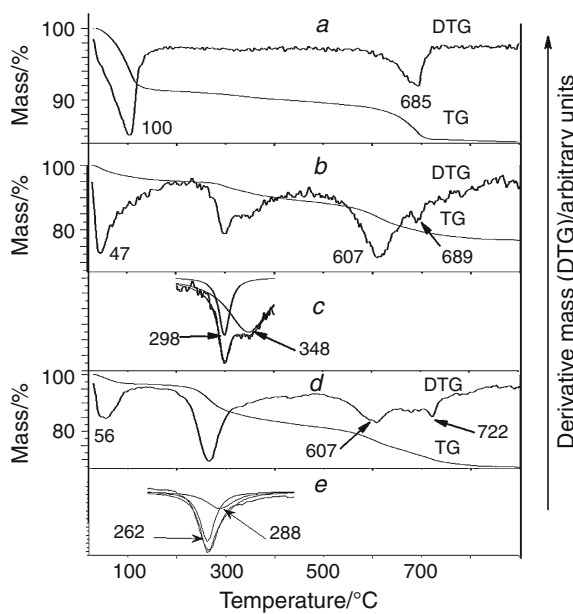


Fig. 1 TG and DTG curves recorded in air of Na-MONT (curves a), OC-41 (curves b and c) and OC-90 (curves d and e). Curves a, b, and d—TG and DTG curves. Curves c and e—fitted DTG curves in the temperature range 175–450 °C

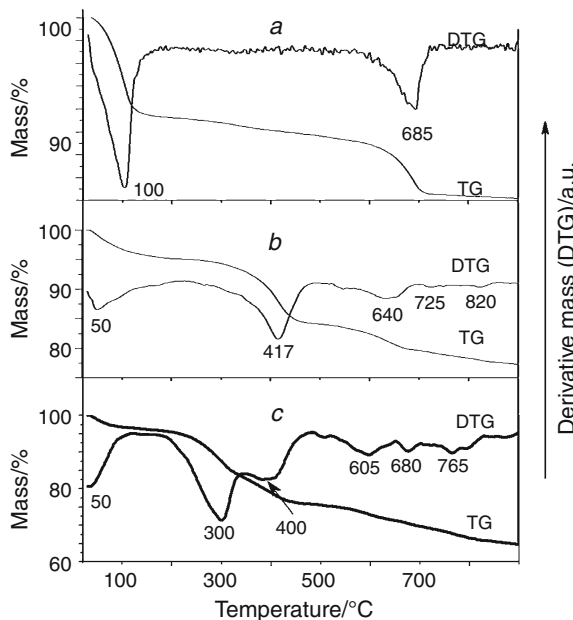


Fig. 2 TG and DTG curves recorded under nitrogen of Na-MONT (curve a), OC-41 (curve b), and OC-90 (curve c)

and NO₂, respectively [15–18, 26]. The non-oxidized carbon and nitrogen form two types of charcoal, one type is oxidized at a lower temperature than the other. According to He, et al. [25] the first DTA exothermic peak which at low HDTMA loadings (46% of the CEC) appeared at 310 °C shifted to 285 °C in the curve of HDTMA–MONT loaded with 96% of its CEC. It is therefore expected that

the air oxidation of adsorbed HDTMA and charcoal formation will start in OC-90 at a lower temperature than in OC-41.

The second and third exothermic peaks at 385–396 and 700–780 °C represent the oxidation of low- and high-temperature stable charcoals, respectively. With increasing loadings the former shifts to lower temperatures and the latter to higher temperatures.

TG and DTG curves

TG and DTG either in air or in inert atmosphere are widely used in the study of organoclays (e.g. [27, 28]). Dweck [29] claimed that TG and DTG curves are more applicable than DTA and DSC curves to identify and analyze the several decomposition steps of natural or synthetic organoclays. DTG curves of Na-MONT used in this study, in air or under nitrogen (curve a in Figs 1, 2), show two peaks at 100 and 685 °C representing dehydration and dehydroxylation of the clay, respectively. The TG curves show that these peaks are associated with mass losses of 8.8% (in the temperature range 25–185 °C) and 4.8% (575–740 °C), respectively. Mass loss in the temperature range 185–575 °C is 2.0%, attributed to the last stage of dehydration and the beginning of the dehydroxylation [15].

TG and DTG curves of OC-41 and OC-90 recorded in air atmosphere are shown in Fig. 1 (curves b and d, respectively) together with the DTG curve fitting calculations in the temperature range 200–450 °C (curves c and e, respectively). The DTG curves together with the fitted DTG curves show five peaks suggesting the presence of five thermal stages of mass loss. In the curve of OC-41 they appear at 47, 298, 348, 607, and 689 °C and in that of OC-90 at 56, 262, 288, 607, and 722 °C. The first DTG peak occurs with the escape of interlayer water. First stage mass losses determined in Na-MONT (25–185 °C), OC-41 (25–185 °C) and OC-90 (25–130 °C) are 8.8, 4.7, and 3.0%, respectively. These results confirm previous studies showing that amounts of interlayer water decrease with increasing clay loadings with organic ammonium cations [15, 30].

The second thermal mass loss stage results from the first oxidation step of the organic cation, the escape of H₂O, CO₂, and NO₂ and the formation of non-volatile intercalated charcoal. The second DTG peak occurs in OC-41 at a higher temperature than in OC-90 in agreement with the DTA study of HDTMA–MONT by He et al. [25] who showed that the first DTA exothermic peak shifted to lower temperatures with increasing loading of the clay. It should be noted that the peak temperatures determined in our study are lower than that determined by He et al. probably due to the fact that our heating rate is 10 °C/min and that of He et al. was faster (20 °C/min).

The third thermal mass loss stage comprises the oxidation of the low temperature stable charcoal leaving the high temperature stable variety in the clay interlayer. Here again the third DTG peak occurs in OC-41 at higher temperature than in OC-90. The fourth mass loss stage (fourth DTG peak) represents the dehydroxylation of the clay. As shown previously, organic-ammonium-MONTs dehydroxylate at temperatures lower than neat Na-MONT [15–18]. The fifth mass loss stage (fifth DTG peak) represents the oxidation of the high temperature stable charcoal.

The TG curves of OC-41 and OC-90 show overlapping of mass loss in the second and third stages on one hand and in the fourth and fifth stages on the other. Mass losses in these overlapping stages are 6.0 and 9.9% in the TG curve of OC-41 and 13.0 and 14.0 in the TG curve of OC-90. Na-MONT shows mass loss in the equivalent temperature ranges 200–450 and 450–800 °C of 1.7 and 5.0%, respectively. The last mass loss of Na-MONT results from the dehydroxylation of the clay. The oxidation of high temperature stable charcoal in OC-41 and OC-90 overlaps the dehydroxylation of the clay. Consequently, the percent of high temperature stable charcoal is determined by subtracting 5.0% from the mass loss occurring in the fourth and fifth stages. It is equal to 4.9 and 9.0% in OC-41 and OC-90, respectively.

Thermal degradation of different organoclays in inert atmosphere was investigated by several investigators [31–36]. Thermal analysis curves of organoclays show stepwise degradation which corresponds to residual water desorption followed by decomposition of the organic modifier and volatilization of organic fragments, dehydroxylation of the clay and the last stages of organic matter degradation and volatilization. Depending on the adsorbed organic species simultaneous TG-EGA showed three, two, and one well-defined degradation stages. It was also observed that the onset of the decomposition was different for each type of organoclay and also depended on whether the organic species was adsorbed on the outside surface or inside the interlayer space, the latter required a higher decomposition temperature. These investigators report that the IR spectra of the evolved gases showed bands related to water, aldehydes, carboxylic acids, aliphatic compounds and in some cases also aromatic compounds and CO₂.

The DTG curve of OC-41 recorded under nitrogen shows five peaks at 50, 417, 640, 725, and 825 °C representing (1) dehydration, (2) thermal degradation of HDTMA cations followed by the escape of volatile fragments and the condensation of nonvolatile fragments into some kind of quasi-charcoal, (3) dehydroxylation of the clay and in the last two stages the pyrolysis of the quasi-charcoal. The TG curve shows that the peaks are associated with mass losses of 4.8% (25–230 °C), 11.0% (230–515 °C), 4.3% (515–700 °C), 2.1% (700–800 °C), and 0.8%, (800–900 °C), respectively.

DTG curve of OC-90 recorded under nitrogen shows seven peaks at 50, 300, 400, 605, 680, 795, and 880 °C representing (1) dehydration, (2, 3) degradation of HDTMA, escape of volatile fragments and condensation of the residue, (4) dehydroxylation of the clay and (5-7) pyrolysis of the quasi-charcoal to volatile fragments. The TG curve shows that the peaks are associated with mass losses of 3.6% (25–160 °C), 13.4% (160–350 °C), 7.0% (350–480 °C), 4.2% (480–655 °C), and 7.2% (655–900 °C), respectively. These results suggest that the type of the quasi-charcoal depends on the initial loading of the HDTMA–MONT.

Carbon and hydrogen chemical analyses

Carbon and hydrogen contents determined in each clay sample by micro analysis before and after thermal treatments are shown by thermo-C and H-analysis curves. In these curves carbon or hydrogen contents (in percentage calculated on the basis of air-dried clay) are plotted against the temperature of the thermal treatment. In Figs. 3 and 4, thermo-C and H-analysis curves of Na-MONT, OC-41, and OC-90 are shown. The thermal treatments were carried out in steps, namely, each sample was heated in an oven under air for 2 h at 150, 250, 360, 420, 550, 700, and 900 °C and was analyzed. This thermal treatment differs from that used in the TG study where the samples were consecutively heated from room temperature to 900 °C. It should be taken in mind that a reaction attributed to a certain DTG peak might be completed in the non-consecutive thermal treatment at a lower temperature.

Before the thermal treatment, the content of carbon in Na-MONT is 1.0% due to the presence of some organic impurities in the Wyoming bentonite. Thermo-Carbon-

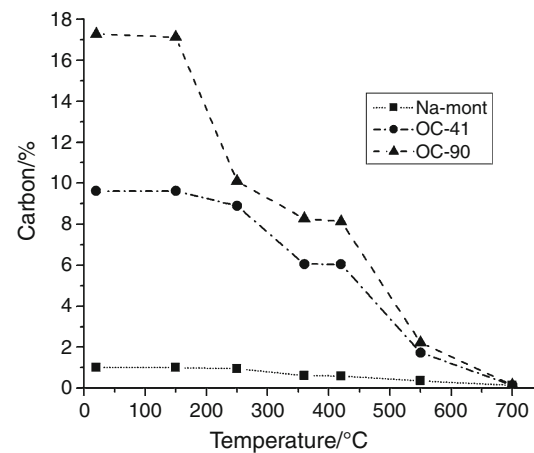


Fig. 3 Carbon analysis curves of Na-MONT, OC-41, and OC-90 showing the content of carbon (in percentage calculated on the basis of air-dried clay) in the different clay samples before and after thermal treatments

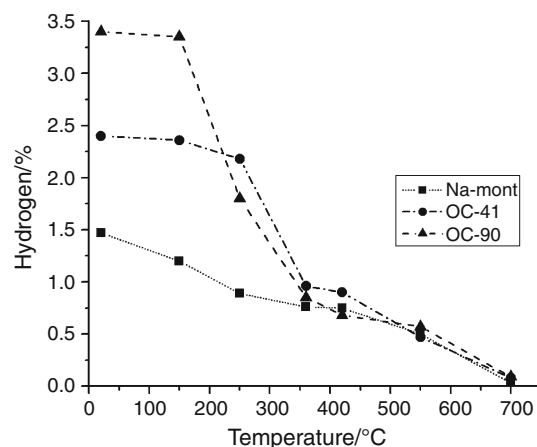


Fig. 4 Hydrogen analysis curves of Na-MONT, OC-41, and OC-90 showing the content of organic and inorganic hydrogen (in percentage calculated on the basis of air-dried clay) in the different clay samples before and after thermal treatments

analysis curve shows very small decreases of 0.1 and 0.3% at 250 and 360 °C, respectively suggesting that the organic matter is oxidized with the evolution of CO₂ and the formation of small amounts of non-volatile charcoal. Further decrease occurs at 550, 700, and 900 °C as a result of charcoal oxidation, leaving 0.4, 0.2, and 0.1% carbon in the clay, respectively.

Carbon contents of unheated OC-41 and OC-90 are 9.6 and 17.3%. Thermo-carbon analysis curves of OC-41 and OC-90 do not show any loss at 150 °C, suggesting that the oxidation of HDTMA occurs at higher temperatures. A small decrease in carbon content (0.7%) occurs in OC-41 at 250 °C. On the other hand, the thermo-carbon analysis curve of OC-90 shows at 250 °C a high decrease of 7.2%. At this temperature oxidation of HDTMA and charcoal formation is significant in the latter, but is very small in the former. After heating at 360 °C, carbon content further drops in OC-41 and OC-90 by 2.8 and 1.8%, respectively. At this temperature oxidation and existence of charcoal is evident in both samples. In agreement with the DTG observations, the present results confirm that OC-90 forms charcoal at a lower temperature than OC-41.

Above 420 °C, there is a constant decrease in carbon content. After 900 °C carbon content in both clays is 0.1%. Carbon loss at 420–900 °C is due to the oxidation of the high temperature stable charcoal [16, 17, 37].

Thermo-hydrogen analysis curve of Na-MONT reveals two stages in the decrease of hydrogen content in the clay. In the first stage, the decrease from room temperature (1.5%) to 360 °C (0.8%) is due to the escape of surface and interlayer water whereas the decrease in the second stage between 420 (0.8%) and 700 °C (0.03%) is due to the dehydroxylation of the clay. No hydrogen is found in Na-MONT heated at 900 °C.

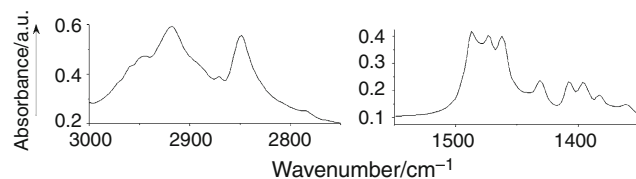


Fig. 5 FTIR spectrum of a KBr disk of neat HDTMA in the spectroscopic regions 3000–2750 cm⁻¹ (left) and 1550–1350 cm⁻¹ (right)

Hydrogen analysis of an organoclay determines simultaneously the quantities of inorganic and organic hydrogen and the hydrogen analysis curves of OC-41 and OC-90 should be treated with caution. During TG runs of Na-MONT with no tetrahedral substitution interlayer water escapes below 205 °C. This is not the case with OC-41 or OC-90. Large organic-ammonium cations break the structure of interlayer water [38] thus interlayer water in HDTMA-MONT is non-structured [39]. Due to the tetrahedral substitution of Si by Al in Wyoming montmorillonite [40], atoms of the oxygen plane become electron-pair donors. Non-structured water molecules form H-bonds with these atoms by donating protons and evolution of water requires higher temperatures than that of the evolution of structured water [41]. The hydrogen analysis curve of OC-41 shows a drastic hydrogen loss at 360 °C but in the curve of OC-90 a drastic loss occurs at 250 °C. The loss is much higher than that observed in Na-MONT and occurs together with a great loss of carbon, suggesting that it originates from oxidation of organic hydrogens. These observations support the conclusion from the TG results that charcoal is formed in OC-90 at a lower temperature than in OC-41.

From 420 °C, the curves of OC-41 and OC-90 overlap that of Na-MONT, suggesting that at this thermal stage the hydrogen which is evolved originates mainly from the clay dehydroxylation.

Thermo-IR-spectroscopy-analysis

Infrared spectrum of a KBr disk of HDTMABr is depicted in Fig. 5. Infrared spectra of KBr disks of MONT complexes of HDTMA (OC-41 and OC-90) non-heated and after heating the organoclays at 150, 250, 360, and 420 °C, in the spectroscopic regions 3000–2750 and 1550–1350 cm⁻¹ are shown in Figs 6 and 7, respectively. Spectra of samples heated at 360 and 420 °C are shown after correcting their baseline by using “Origin 7.0” program. In these spectroscopic regions, the stretching and deformation C–H bands of the organic compounds are found whereas the OH, Si–O, Al–O, and Mg–O absorption bands of the clay framework, as well as those of adsorbed water, are not present. The absorption bands of the C–H vibrations (methyl and ethyl groups) are

Fig. 6 FTIR spectra of KBr disks of OC-41 unheated (curves *a*) and after heating the organoclay at 150, 250, 360, and 420 °C (curves *b*, *c*, *d*, and *e*, respectively) in the spectroscopic regions 3000–2750 cm⁻¹ (left) and 1550–1350 cm⁻¹ (right), after correcting the baselines of curves *d* and *e*. Absorbance scale (in AU) of each curve is given on its left side

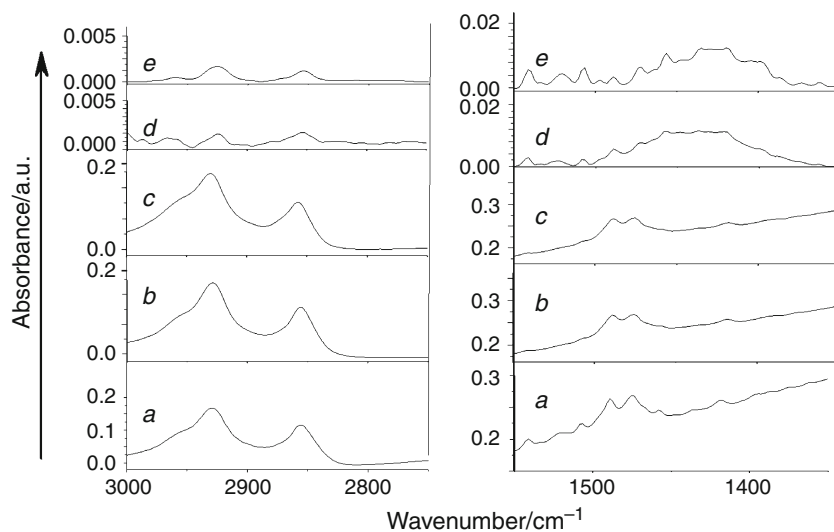
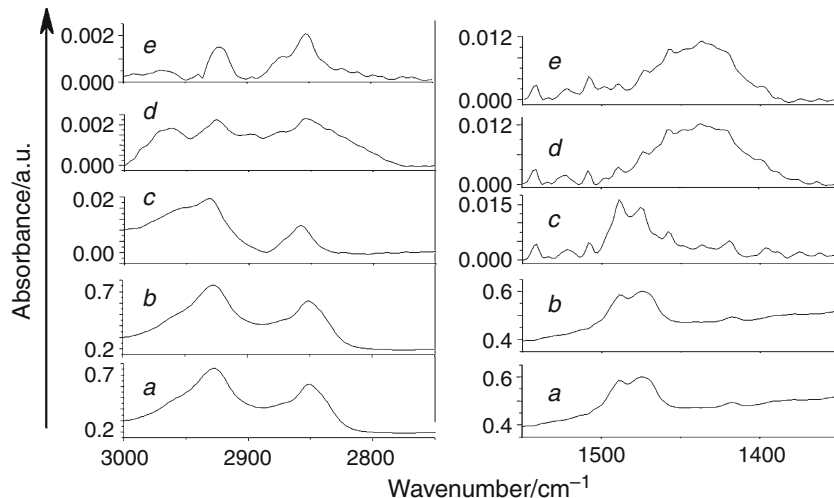


Fig. 7 FTIR spectra of KBr disks of OC-90 unheated (curves *a*) and after heating the organoclay at 150, 250, 360, and 420 °C (curves *b*, *c*, *d*, and *e*, respectively) in the spectroscopic regions 3000–2750 cm⁻¹ (left) and 1550–1350 cm⁻¹ (right), after correcting the baselines of curves *c*, *d*, and *e*. Absorbance scale (in AU) of each curve is given on its left side



extremely weak compared with those of the clay framework bands and using these spectroscopic regions enables to follow after the thermal reactions of the adsorbed organic cations.

Absorption maxima of C–H vibrations in the FTIR spectrum of neat non-heated HDTMABr, and in spectra of OC-41 and OC-90 non-heated and after heating the organoclays at 150, 250, 360, and 420 °C are collected in Table 1 together with their assignments [42]. Frequencies of band maxima of samples heated at 360 and 420 °C were determined after baseline corrections made by using “Origin 7.0” program in the ranges 3000–2750 and 1550–1350 cm⁻¹. The intensities of these bands relative to the most intense CH bands in the specific spectroscopic regions are also noted in the table. These relative intensities are valid only in these narrow regions because in the whole spectrum these bands are extremely weak relative to the clay framework bands.

Table 1 shows that as a result of adsorption by the clay the CH₃ stretching bands of HDTMABr become weak or disappear indicating that in the interlayer space the freedom of the C–H group to vibrate is restricted compared to its freedom before the intercalation. This restriction may be due to keying of the methyl groups into trigonal holes in the clay–oxygen plane. The table also shows that there are small shifts in the asymmetric and symmetric C–H stretching vibrations of the CH₂ group. This is associated with the change of the environment of the *n*-C₁₆H₃₃ chain. In the neat non-adsorbed surfactant there are contacts and van der Waals interactions between parallel chains whereas after adsorption contacts and van der Waals interactions occur between the aliphatic chain and the clay–oxygen plane.

IR spectra shown in curves *d* and *e* in Figs 6 and 7 differ from curves *a*, *b* and *c* suggesting that significant changes occurred at 360 °C. During the thermal treatment the

samples become black and spectra d and e are diagnostic for charcoal, formed during the thermal oxidation of the intercalated HDTMA. In the region 3000–2750 cm⁻¹, where CH vibrations are supposed to appear, the C–H bands in curves d and e are very weak in comparison to their intensities in curves a and b (pay attention that the absorbance scale in curves a and b differs from that in d and e). Three and five very weak bands appear in the spectra of heated OC-41 and OC-90, respectively (Table 1). Their presence suggests that few CH groups exist in the charcoal at 360 and 420 °C. In the region 1550–1350 cm⁻¹ the spectra show five overlapping broad bands with maxima at 1457, 1447, 1437, 1421, and 1399 cm⁻¹ (Table 1). These absorptions of the charcoal skeleton are CC groups resonating between canonic structures with single and double bond character.

Curve c in Fig 6 is very similar to curves a and b. On the other hand, curve c in Fig 7 shows some changes from a and b. In the region 3000–2750 cm⁻¹, the C–H bands in curve c are weak compared to their intensities in curves a and b and the shoulder at 2995 cm⁻¹ becomes more clear. In the region 1550–1350 cm⁻¹, curve c shows small characteristic bands of HDTMA together with small bands of charcoal (Table 1). These observations prove our conclusions based on DTG and thermo-carbon analysis curves that the organic matter in OC-41 requires a higher temperature to become charcoal compared with OC-90. To conclude, the thermo-IR spectroscopy study proves that OC-41 heated at 250 °C contains mainly the non-oxidized HDTMA cations whereas OC-90 heated at 250 °C contains significant amounts of low temperature stable charcoal.

Conclusions

The number of cation exchange sites which are occupied by the organic ammonium cations influences the intergallery confinement of the cation [43]. It is therefore expected that the thermal behavior of OC-90 with the greater number of HDTMA cations occupying exchange sites will differ from that of OC-41. From the TG curves, the thermo-H and C-analysis curves and the thermo-IR-spectroscopy, it may be concluded that HDTMA cations, which are located in the interlayers of OC-41 and OC-90 at room temperature, persist at 150 °C. At 250 °C, most of the HDTMA cations persist in OC-41 and only a very small amount of charcoal is formed. On the other hand in OC-90 at 250 °C a significant part of HDTMA cations are oxidized into low temperature stable charcoal. After heating both samples at 360 °C high temperature stable charcoal is present in both organo clays. Charcoal persists at 420 °C in both clays but is gradually oxidized with further rise in temperature.

Acknowledgements Help from Nadezhda Bukhanovsky (The Volcani Center, Agricultural Research Organization, Israel) in preparing thermally treated organoclays samples is appreciated. This research was supported by a grant from the Israeli Science Foundation (No 919/08) and by a grant from the Ministry of Science, Culture & Sport, Israel & the Ministry of Research (Infrastructure 3-4136).

References

1. Jordan JW. Organophilic clay-base thickeners. In: Proceedings of 10th National Conference on Clays and Clay Mineral, vol 10. Oxford: Pergamon; 1963. p. 299–308.
2. Lagaly G. Interaction of alkylamines with different types of layered compounds. Solid State Ion. 1986;22:43–51.
3. Bergaya F, Lagaly G. Surface modification of clay minerals. Appl Clay Sci. 2001;19:1–3.
4. Ruiz-Hitzky E, Van Meerbeek A. Clay mineral and organoclays-polymers nanocomposites. In: Bergaya F, Theng BKG, Lagaly G, editors. Handbook of clay science. Amsterdam: Elsevier; 2006. p. 583–621.
5. Murray HH. Traditional and new applications for kaolin, smectite, and palygorskite: a general overview. Appl Clay Sci. 2000; 17:207–21.
6. Churchman GJ, Gates WP, Theng BKG, Yuan G. Clays and clay minerals for pollution control. In: Bergaya F, Theng BKG, Lagaly G, editors. Handbook of clay science. Amsterdam: Elsevier; 2006. p. 625–75.
7. Adebajo MO, Frost RL, Kloprogge JT, Carmody O. Porous materials for oil spill cleanup: a review of synthesis and absorbing properties. J Porous Mater. 2003;10:159–70.
8. Ray SS, Okamoto M. Polymer/layered silicate nanocomposites: a review from preparation to processing. Prog Polym Sci. 2003;28: 1539–641.
9. Vianna MMGR, Dweck J, Quina FH, Carvalho FMS, Nascimento CAO. Toluene and naphthalene sorption by iron oxide/clay composites. Part II. Sorption experiments. J Therm Anal Calorim. 2010;101:887–92.
10. Borisover M, Bukhanovsky N, Lapides I, Yariv S. Thermal treatment of organoclays: effect on the aqueous sorption of nitrobenzene on n-hexadecyltrimethyl ammonium montmorillonite. Appl Surf Sci. 2009. doi:[10.1016/j.apsusc.2009.12.133](https://doi.org/10.1016/j.apsusc.2009.12.133).
11. Giese RF, van Oss CJ. Organophilicity and hydrophobicity of organoclays. In: Yariv S, Cross H, editors. Organo-clay complexes and interactions. New York: Marcel Dekker; 2002. p. 175–91.
12. Burstein F, Borisover M, Lapides S, Yariv S. Secondary adsorption on nitrobenzene and m-nitrophenol by hexadecyltrimethylammonium-montmorillonite: thermo-XRD-analysis. J Therm Anal Calorim. 2008;92:35–42.
13. Borisover M, Gerstl Z, Burshtein F, Yariv S, Mingelgrin U. Organic sorbate-organoclay interactions in aqueous and hydrophobic environments: sorbate-water competition. Environ Sci Technol. 2008;42:7201–6.
14. Green-Kelly R. The montmorillonite minerals (smectites). In: Mackenzie RC, editor. The differential thermal investigation of clays. London: Mineralogical Society (Clay Minerals Group); 1957. p. 140–64.
15. Ovadyahu D, Lapides I, Yariv S. Thermal analysis of tributylammonium montmorillonite and Laponite. J Therm Anal Calorim. 2007;87:125–34.
16. Langier-Kuzniarowa A. Thermal analysis of organo-clay complexes. In: Yariv S, Cross H, editors. Organo-clay complexes and interactions. New York: Marcel Dekker; 2002. p. 273–344.

17. Yariv S. Differential thermal analysis (DTA) in the study of thermal reactions of organo-clay complexes. In: Ikan R, editor. Natural and laboratory simulated thermal geochemical processes. Dordrecht: Kluwer Academic Publishers; 2003. p. 253–96.
18. Yariv S. The role of charcoal on DTA curves of organoclays complexes: an overview. *Appl Clay Sci.* 2004;24:225–36.
19. Yermiyahu Z, Landau A, Zaban A, Lapides I, Yariv S. Mono-ionic montmorillonites treated with Congo-red: differential thermal analysis. *J Therm Anal Calorim.* 2003;72:431–41.
20. Yermiyahu Z, Lapides I, Yariv S. Thermo-XRD-analysis of montmorillonite treated with protonated Congo-red: curve fitting. *Appl Clay Sci.* 2005;30:33–41.
21. Sonobe N, Kyotani T, Hishyama Y, Shiraishi M, Tomita A. Formation of highly oriented graphite from poly (acrylonitrile) prepared between the lamellae of montmorillonite. *J Phys Chem.* 1988;92:7029–34.
22. Sonobe N, Kyotani T, Tomita A. Carbonization of polyacrylonitrile in a two dimensional space between montmorillonite lamellae. *Carbon.* 1988;26:573–8.
23. Sonobe N, Kyotani T, Tomita A. Carbonization of poly(furfuryl alcohol) and poly(vinyl acetate) prepared between the lamellae of montmorillonite. *Carbon.* 1990;28:483–8.
24. Sonobe N, Kyotani T, Tomita A. Formation of graphite thin film from poly(furfuryl alcohol) and poly(vinyl acetate) prepared between the lamellae of montmorillonite. *Carbon.* 1991;29:61–7.
25. He H, Ding Z, Zhu J, Yuan P, Xi Y, Yang D, Frost RL. Thermal characterization of surfactant-modified montmorillonite. *Clays Clay Min.* 2005;53:287–93.
26. Yermiyahu Z, Kogan A, Lapides I, Pelly I, Yariv S. Thermal study of naphthylammonium- and naphthylazonaphthylammonium-montmorillonite XRD and DTA. *J Therm Anal Calorim.* 2008;91:125–35.
27. Ni R, Huang Y, Yao C. Thermogravimetric analysis of organoclays intercalated with the Gemini surfactants. *J Therm Anal Calorim.* 2009;96:943–7.
28. Lu L, Cai J, Frost RL. Desorption of stearic acid from surfactant adsorbed montmorillonite. *J Therm Anal Calorim.* 2010;100:141–4.
29. Dweck J. Qualitative and quantitative characterization of Brazilian natural and organophilic clays by thermal analysis. *J Therm Anal Calorim.* 2008;92:129–35.
30. Jordan JW. Alteration of the properties of bentonite by reaction with amines. *Mineral Mag.* 1949;28:598–605.
31. Gao Z, Xie W, Hwu JM, Wells L, Pan WP. The characterization of organic modified montmorillonite and its filled pmma nanocomposite. *J Therm Anal Calorim.* 2001;64:467–75.
32. Xie W, Gao Z, Pan WP, Hunter D, Singh A, Vala R. Thermal degradation chemistry of alkyl quaternary ammonium montmorillonite. *Chem Mater.* 2001;13:2979–90.
33. Xi Y, Martens W, He H, Frost RL. Thermogravimetric analysis of organoclays intercalated with the surfactant octadecyltrimethylammonium. *J Therm Anal Calorim.* 2005;81:91–7.
34. Cervantes-Uc JM, Cauich-Rodriguez JV, Vazquez-Torres H, Grafias-Mesias LF, Paul DR. Thermal degradation of commercially available organoclays studied by TGA-FTIR. *Thermochim Acta.* 2007;457:92–102.
35. Tiwari RR, Khilar KC, Natarajan U. Synthesis and characterization of novel montmorillonites. *Appl Clay Sci.* 2008;38:203–8.
36. Onal M, Sarikaya Y. Thermal analysis of some organoclays. *J Therm Anal Calorim.* 2008;91:261–5.
37. Yariv S. Combined DTA-mass spectrometry of organo-clay complexes. *J Therm Anal Calorim.* 1990;36:1953–61.
38. Heller Kallai L, Yariv S. Swelling of montmorillonite containing coordination complexes of amines with transition metal cations. *J Colloid Interface Sci.* 1981;79:479–85.
39. Yariv S. Wettability of clay minerals. In: Schrader ME, Loeb G, editors. Modern approach to wettability. New York: Plenum Press; 1992. p. 279–326.
40. Yariv S. The effect of tetrahedral substitution of Si by Al on the surface acidity of the oxygen plane of clay minerals. *Int Rev Phys Chem.* 1992;11:345–75.
41. Newman ACD, Brown G. The chemical constitution of clays. In: Newman ACD, editor. Chemistry and composition of clays and clay minerals. Mineralogical society monograph no. 6. London: Longman Scientific & Technical; 1987. p. 1–128.
42. Rao CNR. Chemical applications of infrared spectroscopy. New York: Academic Press; 1963. p. 125–281.
43. Ganguly S, Dana K, Ghatak S. Thermogravimetric study of *n*-alkylammonium-intercalated montmorillonites of different cation exchange capacity. *J Therm Anal Calorim.* 2010;100:71–8.